Research Article

Estimating North Texas Urban Tree Above-Ground Biomass Based on Terrestrial LiDAR and Optimized Quantitative Structure Models

Elizabeth Elkins[1] and Kashif Mahmud[2,*]

[1] Kimbell School of Geosciences, Midwestern State University, Wichita Falls TX 76308, lizcelkins10@gmail.com
[2] Kimbell School of Geosciences, Midwestern State University, Wichita Falls TX 76308, kashif.mahmud@msutexas.edu
[*] Corresponding Author: kashif.mahmud@msutexas.edu; +1-940-397-4475

Abstract: Several studies have revealed that terrestrial light detection and ranging (LiDAR) remote-sensing technology can be an alternative, more accurate approach to estimate tree above-ground biomass (AGB). A set of algorithms has been developed to create a volume reconstruction of tree point clouds, which can be converted to an AGB estimate. These calculate AGB non-destructively and more accurately compared to current forestry practices, which use generic allometric equations. LiDAR scans of trees within Midwestern State University's campus were collected and analyzed with a tree segmentation/modeling algorithm. The validation method was based on comparing the estimated above-ground attributes to actual field measurements. Optimized PD1 and PD2Max increase as the tree size increases, whereas PD2Min remains relatively the same for different tree sizes. Quantitative structure modeling (QSM) produces accurate diameter at breast height (DBH) estimates, however it fails to calculate it precisely when there are low branches or dense leaves within the canopy. These occlusions commonly occur with certain tree species, such as *Pinus echinata* and *Juniperus virginiana*. Our result suggests good agreement of QSM-derived AGB estimates for larger trees but overestimated AGB for smaller trees. This is due to the limitations in LiDAR technology, struggling to accurately scan fine branches and twigs of small trees, leading to errors in point cloud data and subsequent overestimation of their volume in the QSM. While the study provides valuable insights, the small sample size due to the complexity of destructive tree harvesting in urban ecosystems might limit the generalizability of the results.

Keywords: LiDAR, QSM, urban, trees, AGB

Academic Editor: Jeong Chang Seong
Received: 5 May 2025
Revised: 9 July 2025; 5 August 2025
Accepted: 16 August 2025
Published: 24 October 2025

Citation: Elkins, E., & Mahmud, K. (2025). Estimating North Texas Urban Tree Above-Ground Biomass Based on Terrestrial LiDAR and Optimized Quantitative Structure Models. *Journal of Earth Observation and Geospatial Applications*, *1*(1), 94–107. DOI: https://doi.org/10.65372/8w66ep09

1. Introduction

Urban green spaces serve to increase mental health and wellbeing (e.g., Lee *et al.*, 2015), increase air quality (Wolf *et al.*, 2020), reduce heat island effects and provide comfort (e.g., Aram *et al.*, 2019; Rahman *et al.*, 2020), ultimately reducing the energy consumption of buildings (McDonald *et al.*, 2019). Urban vegetation, particularly on university campuses, is a good way to promote stewardship of the environment (e.g., trash pickups, tree planting and adoption, wildlife awareness) and foster community-based events (Schick *et al.*, 2023). Improving the knowledge of tree carbon storage will help better understand climate change, both locally and globally (Nowak & Crane, 2002).

Furthermore, such plantings manage and store carbon, and doing so in urban spaces is one of the most important ways to offset building carbon emissions (Jo & McPherson, 2001) and combat climate change (Tavasoli *et al.*, 2019). Quantifying above-ground biomass (AGB) permits urban planners to assess carbon storage and other ecosystem functions and design more effective strategies in building carbon sinks (Tigges *et al.*, 2016). Improving the overall net carbon budget starts with gathering information about the study site, which could only be feasible with better tree AGB estimates (Nowak & Crane, 2002). The current rate of urbanization causes urban forests to increase in size as a fraction of the total land cover (Hutyra *et al.*, 2014). And as trees account for up to 97% of urban AGB (Davies *et al.*, 2011), it is of great importance to have an accurate prediction of AGB. In traditional forestry practices, allometric relationships are used to convert

diameter at breast height (DBH, measured 1.3 m above the ground) into tree AGB. These methods were developed through destructive harvesting. Many allometric equations have significant uncertainties, particularly for larger trees that can be attributed to (1) limited harvest data, (2) extrapolating the allometric relationship without considering the environment, and (3) measurement errors of tree dimensions (Mascaro *et al.*, 2011; Duncanson *et al.*, 2015). When species-specific allometries are applied, an approximately 35 % underestimation was found for large trees (Calders *et al.*, 2014). The relationship can lead to errors when estimating biomass or volume growth because it is based on limited observation. Extensive destructive sampling is required for accurate species- and ecosystem-specific allometric equations (Roxburgh *et al.*, 2015). Harvesting trees on a large scale may be practical in forested areas; however, it is often not feasible or too costly in urban settings. Conversely, the allometric equations established for forest trees may not apply to urban trees due to variations in the ecosystem (McHale *et al.*, 2009).

Light detection and ranging (LiDAR) sensors have received significant attention for assessing three-dimensional (3D) tree structure and AGB in various ecosystem types. Recent advancements in terrestrial LiDAR offer fine-scale 3D tree point clouds by recording the reflected signal of millions of laser trajectories produced by the instrument. Although LiDAR has been used in forestry for about two decades, recent advances in remote sensing technology and computational power have made it a commonplace tool in the field. Tree attributes can be assessed without any destructive harvesting (Calders *et al.*, 2014). An individual tree point cloud can be separated from the entire LiDAR point cloud, and tree attributes can be estimated using the quantitative structure modeling (QSM) (Raumonen *et al.*, 2013). The method fits cylinders to the 3D point cloud to construct a tree model for each tree, providing detailed information on volume and structure. QSM has been successfully used in different forest ecosystems (Calders *et al.*, 2014; Tanago *et al.*, 2017; Torresan *et al.*, 2018). The method can estimate AGB within 10 % of values determined by destructive harvesting (Calders *et al.*, 2014). The quality of such volumetric tree models is highly dependent on the complexity of the trees, scan acquisition geometry, pattern and settings, and meteorological conditions during the LiDAR scans. Moreover, a set of QSM parameters controls the overall fit of cylinders and the accuracy of the 3D model. Jiang *et al.* (2020) optimized QSM parameters using 160 Australian eucalyptus trees to calculate AGB for plot-scale carbon budget estimation.

This study aimed to apply QSM on terrestrial LiDAR evaluations of a small population of trees within a North Texas urban setting (the campus of Midwestern State University). The trees in this study were modeled and separated into size groups, allowing an evaluation of tree-size influence on model parameters. The accuracy of high-resolution LiDAR data and state-of-the-art tree segmentation algorithms to quantify above-ground volume to estimate AGB of urban trees was evaluated. Analysis explores ways to improve the post-processing computer algorithms based on the fine-scale ground-truth field data. More importantly, the unprecedented details from LiDAR measurements propagate useful tools for forest structure and growth data, with implications on larger scales, such as using satellite-derived data for local/regional forests. This technique provides a non-destructive approach for estimating tree AGB and has real-world impacts on local stakeholders by informing them of the potential of LiDAR technology and data-based practical recommendations for terrestrial carbon stock and sustainable forestry management strategies.

2. Study Area and Data Collection

2.1. Study Area

This study characterized twenty-four individual trees of varying sizes (DBH = 8.2 – 77 cm) and heights (2.5 – 13.5 m) across the Midwestern State University's (MSU Texas) campus, including distributions at Bolin Science Hall in Figure 1a, Sikes Lake in Figure 1b, and Killingsworth Hall in Figure 1c). All trees were scanned using a Leica BLK360 terrestrial laser scanner. An example of LiDAR tree point clouds on the south side of the Bolin Science Hall can be seen in Figure 2. Most of the trees are species native to the Rolling Plains physiographic province or to the larger North Texas region. The study includes one well-adapted

ornamental species, *Acer truncatum*. All the tree species were identified and listed in Table 1 with corresponding densities (x 10^{-3} kg/cm³) gathered from Appendix 11 of Nowak (2024). Scans were completed during the summer of 2023.

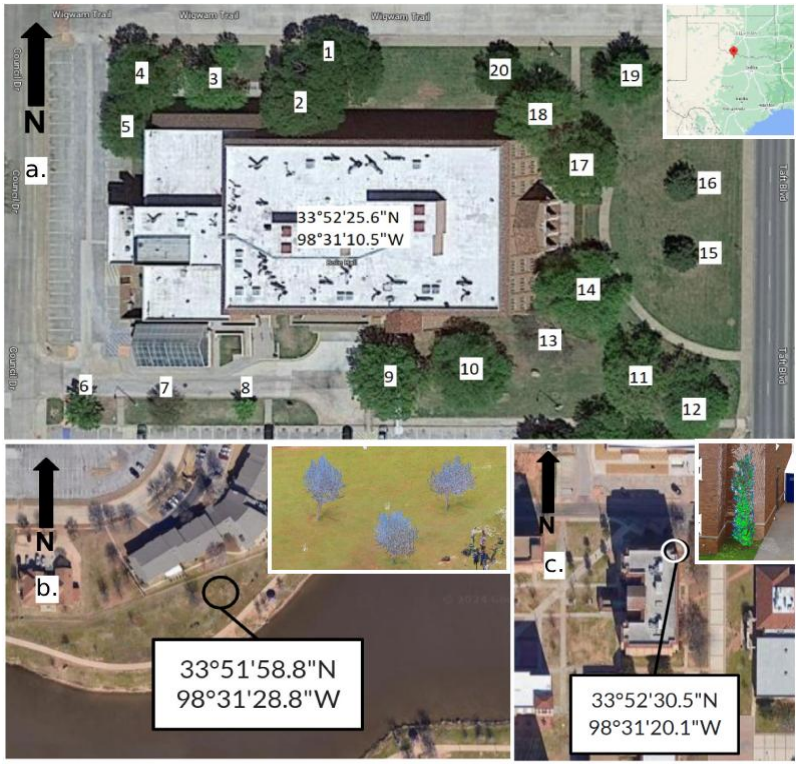

Figure 1. Aerial view of Bolin Science Hall (a), Sikes Lake (b), and Killingsworth Hall (c) with approximate locations (Google Maps). Bolin Science Hall has 20 trees. Sikes Lake has three small trees within the circle, and Killingsworth Hall has one tree within the circle. There are a total of 24 trees. The inset figure in (a) shows the location of MSU Texas' campus. The inset figures in the top right corners (in b & c) show the tree point clouds from LiDAR scans.

Figure 2. Sample LiDAR scan showing tree point clouds on the south side of Bolin Science Hall.

2.2. Data Collection

Field data such as circumference at 1.3 m above ground, LiDAR point clouds, and species were collected for each tree. AGB was measured for four trees, three small (SL1, SL2, SL3) and one large (BO5) (Table 1). The circumference of each tree was measured at the top of a 1.3 m tall wood post reference. The post was

standing upright next to the tree, and the circumference of the trunk was measured using a measuring tape reel. The circumference was converted to diameter (DBH) for each tree. The large tree (BO5, *Ulmus crassifolia*) was weighed on a commercial truck scale. We used Shadman *et al.* (2022) green weight to dry weight equation to obtain the dry weight. The small trees (SL1, SL2, SL3, *Acer truncatum*) were weighed using a standard, hand-held luggage scale. Two trees (SL1 and SL3) were sufficiently small to be weighed intact; the other (SL2) was cut into pieces, where each piece was weighed, and all the weights were summed for the total. All small trees had died prior to harvest, resulting in a dry weight. Species were identified for all 24 trees. LiDAR scans were taken using a Leica BLK360 terrestrial laser scanner at its finest spatial resolution (~3 cm). Capturing a single tree requires multiple scans from different angles. Over 50 scans were captured to survey the entire study area. Every angle of the trees needs to be scanned to have enough data points for accurate modeling. A minimum of four scans per individual tree was obtained. However, the proximity of the trees allows each tree to share multiple scans with the neighboring tree due to the LiDAR scanning in a full 360° rotation. These scans are positioned in the corners of a square around the tree, with the tree in the center.

Table 1. List of the trees considered in this study with their species, common names, density, and size.

Tree ID	Species	Common Name	Density (x 10 kg/cm³)	Tree Size
BO1	*Ulmus crassifolia*	Cedar Elm	0.59	Large
BO2	*Ulmus crassifolia*	Cedar Elm	0.59	Medium
BO3	*Ulmus crassifolia*	Cedar Elm	0.59	Medium
BO4	*Ulmus crassifolia*	Cedar Elm	0.59	Large
BO5	*Ulmus crassifolia*	Cedar Elm	0.59	Large
BO6	*Quercus buckleyi*	Texas Red Oak	0.62	Small
BO7	*Quercus virginiana*	Live Oak	0.8	Medium
BO8	*Quercus buckleyi*	Texas Red Oak	0.62	Small
BO9	*Quercus macrocarpa*	Bur Oak	0.58	Large
BO10	*Ulmus crassifolia*	Cedar Elm	0.59	Medium
BO11	*Quercus buckleyi*	Texas Red Oak	0.62	Large
BO12	*Ulmus crassifolia*	Cedar Elm	0.59	Large
BO13	*Ulmus crassifolia*	Cedar Elm	0.59	Medium
BO14	*Ulmus crassifolia*	Cedar Elm	0.59	Large
BO15	*Pinus echinata*	Shortleaf Pine	0.47	Small
BO16	*Pinus echinata*	Shortleaf Pine	0.47	Medium
BO17	*Ulmus crassifolia*	Cedar Elm	0.59	Large
BO18	*Ulmus crassifolia*	Cedar Elm	0.59	Large
BO19	*Ulmus crassifolia*	Cedar Elm	0.59	Medium
BO20	*Ulmus crassifolia*	Cedar Elm	0.59	Small
SL1	*Acer truncatum*	Shantung Maple	0.59	Small
SL2	*Acer truncatum*	Shantung Maple	0.59	Small
SL3	*Acer truncatum*	Shantung Maple	0.59	Small
KH1	*Juniperus virginiana*	Red Juniper	0.44	Medium

3. Methods

3.1. QSM Derived Tree Attribute

After the LiDAR survey, all individual scans were downloaded using the software Cyclone Register 360 associated with the BLK360 scanner and assembled into a single point cloud. Any unnecessary portions (e.g., buildings, cars, ground) were removed, and each tree point cloud was separated using CloudCompare, a 3D point cloud processing software.

Volume reconstructions of tree point clouds were made using QSM of Raumonen *et al.* (2013). A brief summary of the algorithm is provided below; readers are directed to the source for further details. QSM uses cylinders as basic building blocks to reconstruct the tree model from a point cloud, which is usually produced by a terrestrial laser scanner and must contain only one tree. The tree model is defined based on three parameters (PD1, PD2Min, PD2Max), and optimization of these parameters is imperative for a better representation of the tree. Initial processing of QSM filters the point cloud by creating spheres around the data points and then rejecting those points that contain too few data points within the sphere. This effectively removes noise, reducing the data to the surface of the tree. Next, the cover sets create connected surface patches, defining the surface topology and shape of the tree. The cover sets connect together via neighbor-relation, group data points based on their common point. The number of neighbors typically varies. Once grouped, the algorithm characterizes the cover sets geometrically. Trunk and branches tend to be locally cylindrical, such that the algorithm works best for trees. The branches are separated using the branching relations of the child and parent branches. Finally, the algorithm estimates DBH, surface area, volume, and other geometric attributes. DBH was estimated by taking the diameter of the cylinder at 1.3 m from the ground. Volume measurements were estimated by calculating and summing the volume of the corresponding cylinders.

Jiang *et al.* (2020) used QSM with a set of optimum parameters (PD1 = 0.09, PD2Min = 0.02, and PD2Max = 0.08) based on Australian eucalyptus trees. PD1, PD2Min, and PD2Max control the overall fit of cylinders and the accuracy of QSM. The initial QSM analysis in this study used the Jiang *et al.* (2020) parameters. In subsequent analyses, the parameters were further optimized by comparing field observations of tree weight and DBH within our study area. Different sets of parameters were compared using the Mean Squared Error (MSE) of DBH and harvest AGB. The automated optimization technique within the QSM was first implemented to find the optimum parameters, however it didn't perform well for the trees in this study. Hence, we tried an iterative optimization technique with trial and error and cross-validation. The parameters were composed of numbers ranging from 0.001 to 0.2 for PD1, PD2Min, and PD2Max. Each combination was run on test trees for each size group. The test trees were SL1 and SL2 for the small group; BO2, BO7, and BO19 for the medium trees; and BO5 for the large trees. Test trees for the small and large groups were chosen because their DBH and AGB were known. The medium test trees were chosen at random since there was no known AGB data for this group. The species-specific wood densities from Nowak (2024) were used in this study and are listed in Table 1. QSM-derived volume estimate was multiplied by the wood density to convert to AGB. The model-derived DBH and AGB estimates were compared to the measured DBH and destructively harvested AGB respectively, by calculating error percentage (*((QSM-derived estimate − Field measurement) / Field measurement * 100*) and root mean square errors (RMSE) to assess QSM's performance. Figure 3 compares the LiDAR point cloud and the QSM 3D model with optimum parameters for two (BO11 and BO8) of the Texas Red Oaks from the study area.

3.2. Allometry-based AGB Estimation

The allometry-based AGB was estimated using the equation (Equation 1) from Jenkins *et al.* (2004), where bm = total AGB (kg) for trees with 2.5 cm and larger DBH, DBH = diameter at breast height (cm), β_0 and β_1 are coefficients.

$$bm = \mathrm{Exp}(\beta_0 + \beta_1 \ln(DBH)) \quad (1)$$

The coefficients β_0 and β_1 vary with tree species. This equation is based on compiling published diameter-based allometric regression equations for estimating dry weight AGB (e.g., Gholz *et al.*, 1979; Binkley, 1983) and modifying them using meta-analysis to create a consistent AGB regression equation (Jenkins *et al.*, 2003). Table 2 shows selected parameters. Jenkins *et al.* (2004) suggests using the mixed hardwoods coefficients for Cedar Elm (*Ulmus crassifolia*, the hard maple coefficients for Live Oak (*Quercus virginiana*), the hard maple coefficients for Bur Oak (*Quercus macrocarpa*), the pine coefficients for Shortleaf Pine (*Pinus echinata*), and the cedar coefficients for Eastern Red Cedar (*Juniperus virginiana*). For Texas Red Oak (*Quercus buckleyi*), Jenkins *et al.* (2004) did not directly state which parameters to use. Shumard Oaks (*Quercus shumardii*) are similar to Texas Red Oaks (Greene *et al.*, 2008); therefore, the hard maple parameters are used. Jenkins *et al.* (2004) did not directly state which parameters to use with the Shantung Maple (*Acer truncatum*), but given that the species is a hard maple, those parameters seemed most suitable.

Table 2. The parameters (β_0 and β_1) for the allometry-based estimate for the groups of trees at the study sites (Modified from Jenkins *et al.*, 2004).

Species Group	β_0	β_1	Max DBH (cm)	R^2
Mixed Hardwood	−2.4800	2.4835	56	0.980
Hard Maple	−2.0127	2.4342	73	0.988
Cedar	−2.0336	2.2592	250	0.981
Pine	−2.5356	2.4349	180	0.987

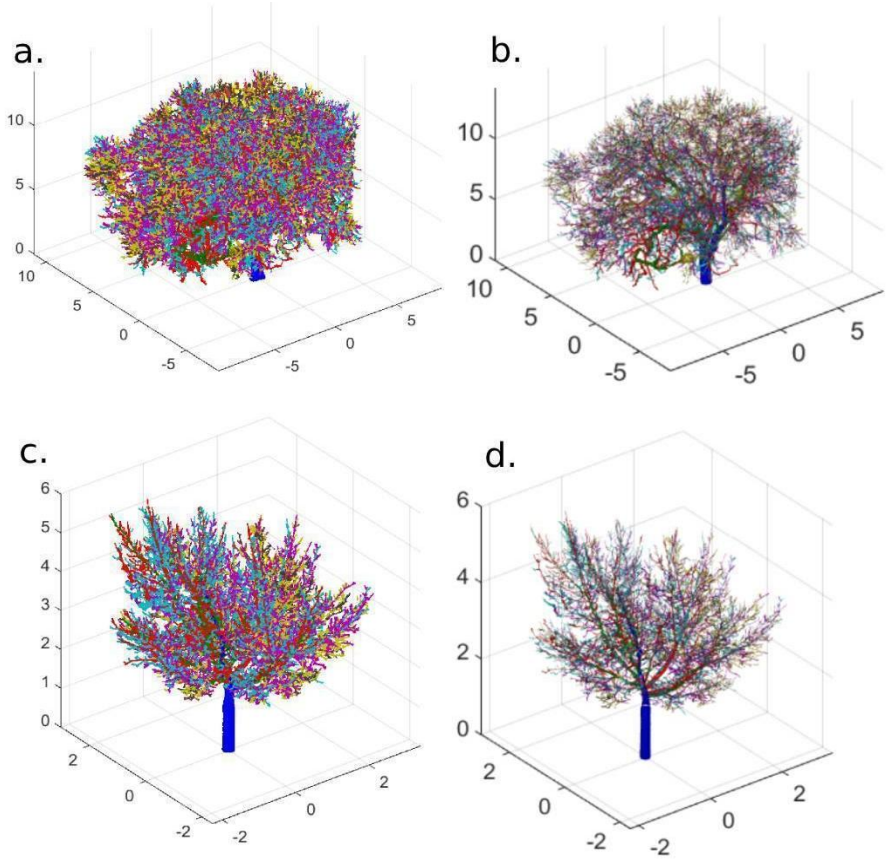

Figure 3. The left column shows BO11 (a) and BO8 (c) point clouds. The right column shows the 3D model generated by QSM for BO11 (b) and BO8 (d). BO11 is located on the southeast side of Bolin Science Hall, and BO8 is located on the southwest side of Bolin Science Hall.

4. Results

4.1. Parameter Optimization

Figure 4 shows the MSE of DBH and harvest biomass (depending on tree groups) for the parameter tests for each parameter (PD1, PD2Min, and PD2Max) and size group (small: DBH < 36 cm, medium: DBH 36 - 55 cm, large: DBH > 55 cm). We used harvested biomass to optimize parameters for both small and large trees, hence the reported MSE values are for biomass and greater than the medium-sized trees. DBH is used for medium-sized trees due to a lack of harvest data. Therefore, the MSE values are for DBH. The small group was optimized using the trunk volume of SL1 and SL2 due to the high error percentage of QSM's total volume estimates. The medium group was optimized using DBH from BO2, BO7, and BO19. These trees were picked because their field DBH measurements were close to the maximum, minimum, and mean of the medium trees' DBH. The large group was optimized using BO5 because we had harvested above-ground mass to compare to QSM's AGB. The figure also plots the computational time required for the corresponding tests. The lowest observed MSE values largely correspond with smaller parameters, and the fastest run times usually occur for larger parameters. There is a trade-off between these two variables in terms of choosing the optimum set of parameters.

For the small trees, the lowest MSE occurred when PD1 = 0.02 with a run time of about 5 minutes. A reduced run time can be achieved, but at the expense of a lower MSE. For PD2Min, the lowest MSE was when PD2Min = 0.01 with a run time of about 13 minutes. For PD2Max, the lowest MSE was at PD2Max = 0.01, having a run time of about 17 minutes. For the medium trees, the parameters do not largely affect the DBH outputs as seen by the relatively consistent MSE values. PD1 was 0.05 with the lowest run time of about 30 hours. For the PD2Min, the lowest MSE was when PD2Min = 0.01 with a run time of about 35 hours while the best run time was when PD2Min = 0.05 at 3 hours. When PD2Min was 0.02, the MSE was slightly higher than PD2Min at 0.01; the slightly higher run time at PD2Min = 0.05 suggested that PD2Min = 0.02 was a better choice. PD2Max = 0.01 produced the lowest MSE for the medium trees for a run time of about 120 hours. The lowest run time was about 15 hours when PD2Max = 0.09. The optimum was when PD2Max = 0.05 because the MSE was similar to the lowest and the run time was about 25 hours. For the large tree, the PD1 = 0.11 yielded the lowest MSE and a lower run time, making it preferable. When PD2Min = 0.01, the MSE was lowest and had a decent run time. PD2Min = 0.03 could be chosen if a shorter run time was preferred. The lowest MSE for PD2Max had a run time of about one hour. However, the shorter run times had increases in MSE. We chose the optimum values for PD2Max to be 0.17 for the large trees.

To summarize, the optimum parameters are listed in Table 3 for three different tree size groups. PD1 and PD2Max increase as the tree size increases, whereas PD2Min remains relatively the same for different tree sizes (Table 3).

Table 3. The optimized parameters for each tree size group.

	Small Group	Medium Group	Large Group
PD1	0.02	0.05	0.11
PD2Min	0.01	0.02	0.01
PD2Max	0.01	0.05	0.17

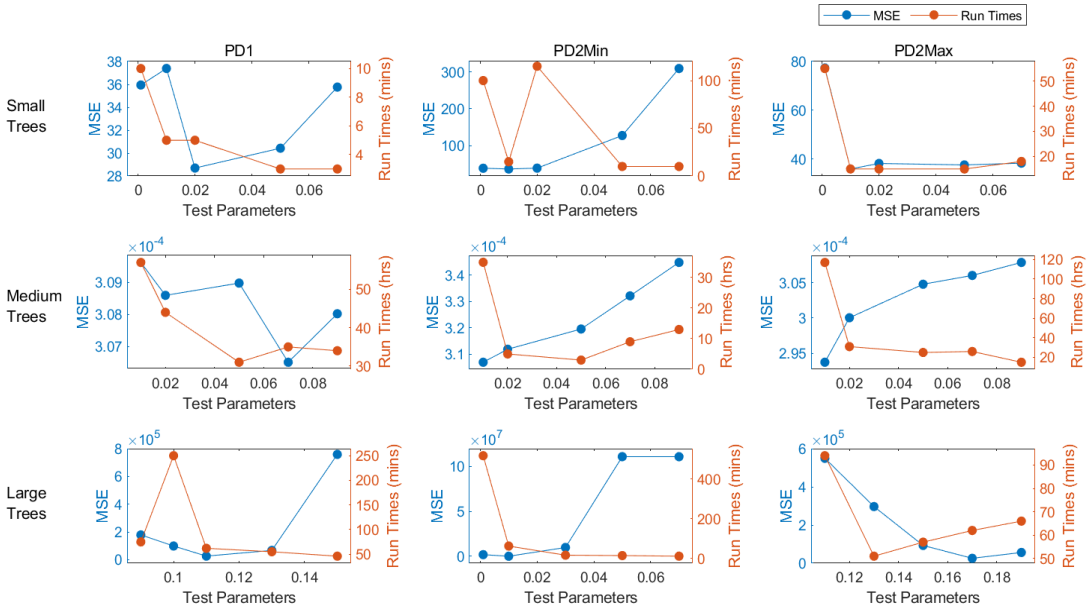

Figure 4. MSE of DBH and harvest biomass for the parameter tests for each parameter (PD1, PD2Min and PD2Max) and size group (small: DBH < 35 cm, medium: DBH 36 – 55 cm, large: DBH > 55 cm) are shown in blue colors. The run times for the corresponding tests are shown in orange colors.

4.2. Evaluation of Tree DBH and AGB

Using the optimized parameters, we calculated the DBH, above-ground volume, and other attributes for all tree point clouds. Table 4 compares measured DBH and AGB versus QSM derived DBH and AGB with the error percentage. The table also lists allometry-based AGB and the difference between the two AGB estimates (QSM-derived vs allometry-based AGB). It also has the total AGB and the total carbon stored in all 24 trees calculated by both methods (QSM-derived and allometry-based). We used half of the dry weight as total carbon storage in these trees (Shadman *et al.*, 2022). QSM and allometry-based AGB error percentages are all positive for smaller trees (SL1, SL2 and SL3) with the exception of the large tree (BO5) having the allometry-based AGB underestimated (Table 4). On the contrary, most of the QSM-derived DBH errors are negative (Table 4), indicating an overall underestimation of DBH prediction. Moreover, the QSM-derived AGB is larger compared to allometry-based AGB estimates (Table 4). For the smaller trees (SL1, SL2, and SL3), the allometry-based AGB had a smaller error percentage compared to the QSM-based AGB (Table 4). For the large tree (BO5), the QSM-derived AGB had a smaller error percentage than the allometry-based AGB (Table 4). The R-squared value of field DBH compared to QSM-derived DBH is 0.95 (Figure 5). The linear regression line has a close match with the 1:1 (major diagonal) line, representing a good agreement between QSM-derived DBH and field DBH. The QSM performed well in calculating the DBH with an overall underestimation and a couple of exceptions (Figure 5). However, the QSM-derived AGB was overestimated significantly (Figure 5) for at least two small trees, with an error of more than 250% (Table 4).

Separate box plots were constructed showing the QSM-derived DBH error percentages for tree size and tree species (Figure 6). The small trees performed well with QSM-derived DBH error ranging from −14.5 to +9.3%, with an RMSE of 3.03 cm, but the medium and large trees had slightly higher error percentages with the medium tree group having the largest variation in the DBH estimates (Figure 6). However, the large tree group had the best match for QSM-derived DBH with the lowest RMSE of only 1.48 cm. When the trees are grouped by species, the cedar elms have an RMSE of 2.77 cm while the oaks have an RMSE of 1.42 cm. The

RMSE on pines was 5.88 cm, and the juniper was 20.92 cm, larger than those for cedar elms and oaks. Overall, the QSM-derived DBH consistently underestimated DBH.

Figure 7 illustrates the differences between the traditional method (allometry-based AGB) and QSM-derived AGB for tree size and tree species. When the AGB difference is grouped by tree genus, most of the QSM-derived AGB estimates for each species group were larger than the corresponding traditional estimates based on allometric equations (Figure 7). The cedar elms have a 75% difference. The oaks and pines both have a 60% difference. However, the juniper (KH1) provided a larger allometry-based AGB than the QSM-derived estimate (460% difference). The average percentage difference between QSM and allometric AGB estimates was 50% when excluding KH1 and 70% when including KH1. These substantial variations between the two techniques indicate the importance of further research, particularly with more harvest data for urban trees.

Table 4. Field measurements, QSM attributes, DBH error, AGB error, and AGB differences between QSM and allometry-based estimates.

Tree ID	Field DBH (cm)	QSM DBH (cm)	DBH Error (%)	Field AGB (kg)	QSM-derived AGB (kg)	AGB Error (%)	Allo. based AGB (kg)	Allo. & QSM based AGB Difference (%)
BO1	74.49	72.00	−3.34	–	5332.64	–	3734.71	−29.97
BO2	50.61	48.06	−5.04	–	3998.37	–	1430.47	−64.22
BO3	45.52	43.31	−4.86	–	2704.14	–	1099.23	−59.35
BO4	58.89	56.00	−4.91	–	4481.68	–	2083.68	−53.51
BO5	61.12	55.00	−10.01	4269	4307.65	0.9	2285.01	−46.95
BO6	30.88	29.00	−6.09	–	527.50	–	564.89	7.09
BO7	37.24	35.55	−4.54	–	5455.75	–	891.54	−83.66
BO8	23.56	23.00	−2.38	–	253.35	–	292.31	15.38
BO9	71.3	70.00	−1.82	–	4868.78	–	4332.50	−11.01
BO10	49.98	47.99	−3.98	–	5153.82	–	1386.20	−73.10
BO11	77.03	75.00	−2.64	–	6290.44	–	5229.35	−16.87
BO12	52.52	51.00	−2.89	–	6413.59	–	1568.31	−75.55
BO13	35.65	35.13	−1.46	–	2731.63	–	599.16	−78.07
BO14	64.94	62.00	−4.53	–	7827.43	–	2656.30	−66.06
BO15	32.79	32.00	−2.41	–	666.78	–	388.49	−41.74
BO16	35.65	27.37	−23.23	–	1290.62	–	476.39	−63.09
BO17	53.16	52.00	−2.18	–	3650.66	–	1615.94	−55.74
BO18	58.57	55.00	−6.10	–	4258.72	–	2055.82	−51.73
BO19	44.88	45.14	0.58	–	5308.29	–	1061.44	−80.00
BO20	29.29	32.00	9.25	–	1766.71	–	367.60	−79.19
SL1	8.19	7.00	−14.53	15.17	56.96	275.45	22.34	−60.78
SL2	9.71	10.00	2.99	30	37.67	25.57	33.81	−10.25
SL3	9.29	8.00	−13.89	16.1	77.27	379.95	30.36	−60.71
KH1	46	25.08	−45.48	–	133.32	–	747.00	460.29
Total AGB (kg):					77593.77		34952.85	
Total Carbon Storage (kg):					38796.89		17476.43	

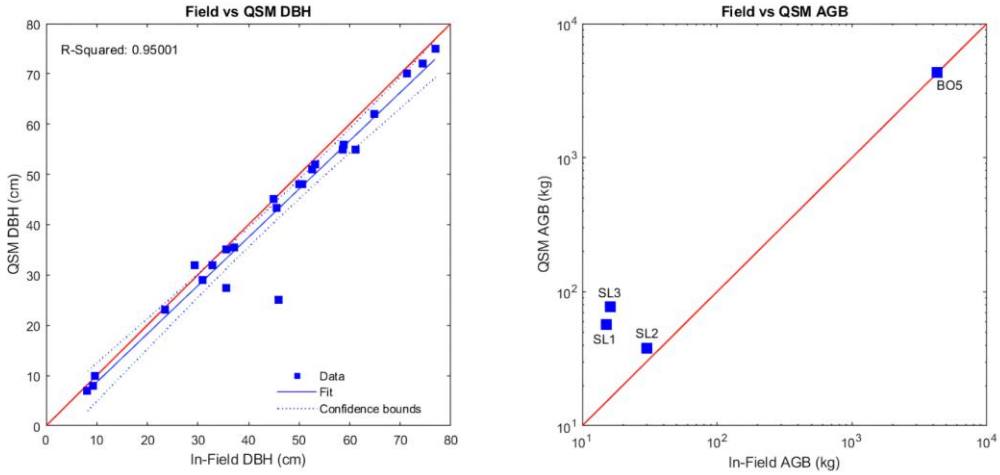

Figure 5. Comparison between field measurements and QSM-derived measurements for both DBH and AGB. We only have four of the trees (BO5, SL1, SL2 and SL3) harvested, hence only four points for the AGB plot. The red line is the 1:1 line. The R-squared and the linear regression line are also shown for the DBH plot.

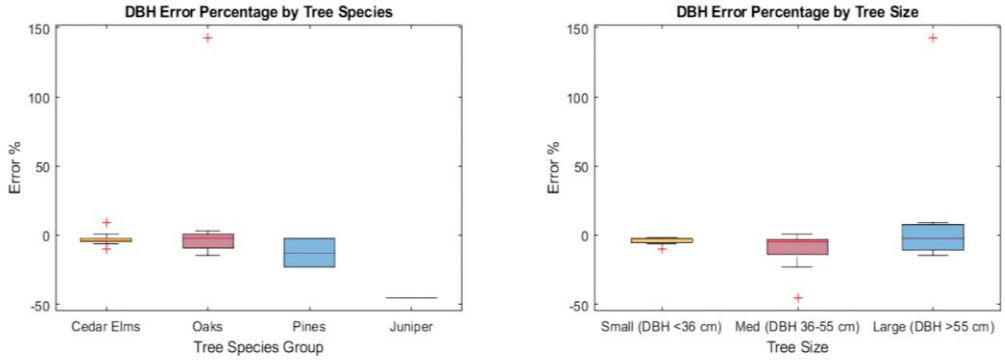

Figure 6. Box plots showing the error percentage for QSM-derived DBH grouped by tree species and size. There are 13 cedar elms, 8 oaks, two pines, and one juniper.

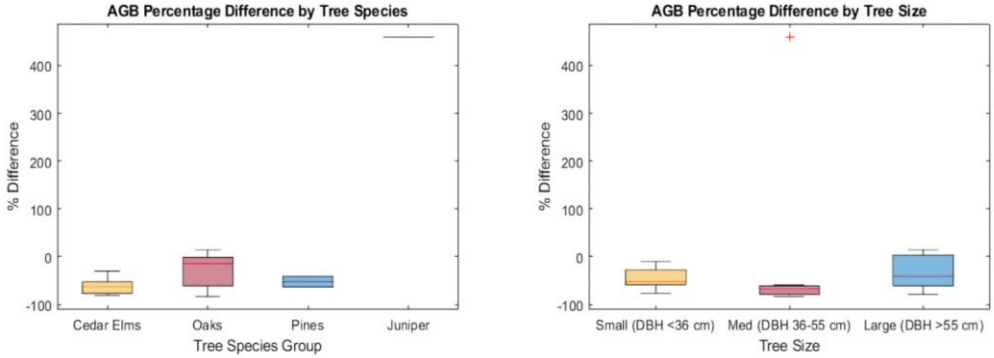

Figure 7. Box plots showing the percentage difference for AGB estimated by two methods (QSM and allometry-based) grouped by tree species and size. There are 13 cedar elms, 8 oaks, two pines, and one juniper.

5. Discussion

5.1. Overview

Generally, QSM is accurate when calculating DBH; it tends to poorly calculate DBH when there are low branches or many leaves. Two trees (BO16 and KH1) had low branches and many leaves, deteriorating the QSM model and DBH estimates. One of the pine trees (BO16, *Pinus echinata*) has many occlusions caused by shadowing due to its low branches and many leaves along the branches. The Juniper tree (KH1, *Juniperus virginiana*) presented issues as well. This tree was in the corner of a building, leading to an insufficient LiDAR scan angle between the building and the tree. KH1 is a tall tree with a narrow shape, and dense branches and leaves distribution. Since the point density in the LiDAR scan was low, QSM had challenges, particularly in reconstructing the stem and branches of the Juniper. Moreover, measuring DBH over bark can lead to significant errors, particularly in younger trees where bark is a larger proportion of the stem, and also in older trees where bark thickness is often variable around the stem. We believe this caused an overestimation of our field DBH measurements, hence the QSM-derived DBH underestimation is expected for these urban trees having irregular bark.

Unfortunately, we have a limited sample size and harvest AGB data, but we found similar results in AGB estimates as previous studies applying QSM (Calders *et al.*, 2014; Tanago *et al.*, 2017; Kükenbrink *et al.*, 2021). Among the four trees with field AGB data, the large tree's (BO5) QSM-derived AGB (4308 kg) was very close to the harvest biomass (4269 kg). However, the traditional allometry-based AGB underestimated the tree by 47%. Allometry-based tree AGB estimation, while a useful tool, can be inaccurate due to several factors. These include the application of equations developed for one species or location to different species or environments, the variability in tree growth patterns influenced by factors like site productivity, and the difficulty in capturing the complexity of tree architecture with simple models. Additionally, small sample sizes in some allometric equations can lead to bias and measurement errors. Hence, QSM offers a non-destructive approach to estimating AGB more accurately than the traditional allometric method, particularly for large trees. We emphasize that accurately estimating the AGB for large trees is vital because of their crucial role in carbon storage within urban forests. They store significantly more carbon than smaller trees, and their size allows them to absorb carbon more efficiently. Large trees accumulate substantial amounts of carbon annually. Protecting and allowing large trees to continue growing is vital for climate mitigation, as they can store carbon within the urban environment for centuries. The accurate prediction of large urban tree biomass directly impacts the estimation of how much carbon is stored and how much is being sequestered annually. Therefore, combining remote sensing techniques with QSM provides an efficient tool for the accurate prediction of carbon storage for urban ecosystems.

QSM-derived AGB overestimated all three smaller trees (SL1, SL2, and SL3) estimates. These overestimations in smaller tree AGB are particularly caused by the tiny branches and twigs, due to limitations in LiDAR technology. Specifically, LiDAR struggles to accurately scan fine branches and twigs, leading to errors in point cloud data and subsequent overestimation of their volume in the QSM, hence the tree AGB. This could also be due to errors within the point clouds, such as occlusions caused by shadowing, movement of the tree during scanning, non-circular branches, non-wooden material, or segmentation and structure errors in the QSM cylinder model (Krooks *et al.*, 2014). For example, one of the small trees (SL1) harvested AGB was 15.17 kg while the QSM estimate was 56.99 kg with an error of 275%. However, the harvest weight of the small trees was measured using a standard luggage scale, which possibly introduced human measurement errors, causing higher error percentages for the small trees. On the contrary, the traditional method performed well in estimating the urban small tree AGB, indicating these equations are derived with adequate field data representing the tree species. However, that is certainly not the case for the large urban tree due to limited harvest data.

This project defined the nature of tree-carbon storage in urban environments. Due to having four AGB ground truth data, more harvest data needs to be collected. This is the starting point for collecting carbon storage data using LiDAR and QSM at MSU Texas campus and for the entirety of the surrounding city,

representing the North Texas urban ecosystem. However, QSM using tree LiDAR point clouds looks promising with better AGB estimation for large urban trees, which is crucial for accurately estimating their role in carbon uptake and storage within cities.

5.2. Future Work

Our work is limited to four samples due to the complexity we faced with destructive tree harvesting in urban ecosystems. It is more common to harvest large forest trees for timber production and forest management for wildlife and ecosystem health, rather than in urban areas. Hence, we chose our campus for the project having the collaboration of the facilities services, informing us before harvesting any campus tree. Due to the small sample size, future work will focus on scanning and harvesting more trees. This will provide more harvest AGB for better parameter optimization for different sizes and species of urban trees. Collecting more harvest data is the most important strategy for creating an accurate estimation of urban carbon storage. Future projects could then include the use of airborne and/or satellite LiDAR to expand the spatial coverage of the study area. QSM can also be used to test allometric equations, particularly for larger trees, which are underrepresented in allometric equations because of limited harvest data (Tanago *et al.*, 2017).

QSM has been further modified recently, with the segmentation process becoming automated. Therefore, modeling has improved with add-ons such as TLS2Trees (Wilkes *et al.*, 2023) and Real Twig (Morales & MacFarlane, 2024). TLS2Trees automatically separates individual tree point clouds. This reduces time spent manually separating trees. Real Twig uses branch measurements to correct QSM models by fixing the volume overestimation commonly found in QSM estimates due to small branches. Using these in future work could greatly improve the accuracy of QSM, especially for the smaller trees and the estimation of total carbon storage in urban ecosystems.

6. Conclusions

Allometric equations are the traditional method to estimate AGB, but they are generalized and based on destructive harvest data. With the advancement of LiDAR technology, assessing 3D tree structure is a feasible method to estimate AGB in various ecosystems including urban environments. The aim of the project was to apply QSM using terrestrial LiDAR data on a small population of trees within a North Texas urban setting. We optimized QSM's parameters (PD1, PD2min, and PD2max) by comparing field data and estimated the total carbon stored in the study site. These optimized parameters vary with tree size. PD1 and PD2max increased as DBH increased, however PD2min stayed the same. Overall, QSM underestimates DBH within 10% when excluding BO16 and KH1. This underestimation is partly due to a possible overestimation in our field measurements due to irregular tree bark. It is evident that the traditional allometry-based equation underestimates the large urban tree AGB by 50%, whereas the QSM-derived AGB has an accurate match with the harvest data (Table 4). Therefore, LiDAR could possibly provide a reasonable evaluation of AGB for urban trees, especially for the large trees, but more data is needed to fully validate this method. The QSM approach is an accurate, most importantly, a non-destructive process to estimate large urban tree AGB and other attributes. Effectively modeling tree characteristics allows for more information about green spaces to be readily available and practically utilized.

Data Availability Statement: Individual tree point clouds, field data, and QSM code can be accessed at https://github.com/liz-elkins/MSUTX-TreeQSM.

Acknowledgment: The authors thank Midwestern State University and AmericaView for supporting this research. This research was funded by Midwestern State University and AmericaView. This material is based upon work supported by the U.S. Geological Survey under Grant/Cooperative Agreement No. G18AP00077 (for GY18-GY22) or G23AP00683 (GY23-GY27). We also thank Dr. Jonathan D. Price and Dr. Steven Rosscoe for their valuable suggestions and Dr. Timothy Pegg for his help with identifying tree species.

Special thanks to Kathryn Brown and Rowann Remie for their help in the field.

Conflicts of Interest: The authors declare no conflicts of interest. The funders had no role in the design of the study; in the collection, analyses, or interpretation of data; in the writing of the manuscript; or in the decision to publish the results.

References

Aram, F., Higueras García, E., Solgi, E., & Mansournia, S. (2019). Urban green space cooling effect in cities. *Heliyon, 5*(4), e01339. https://doi.org/10.1016/j.heliyon.2019.e01339

Binkley, D. (1983). Ecosystem production in Douglas-fir plantations: Interaction of red alder and site fertility. *Forest Ecology and Management, 5*(3), 215–227. https://doi.org/10.1016/0378-1127(83)90073-7

Calders, K., Newnham, G., Burt, A., Murphy, S., Raumonen, P., Herold, M., Culvenor, D., Avitabile, V., Disney, M., Armston, J., & Kaasalainen, M. (2014). Nondestructive estimates of above-ground biomass using terrestrial laser scanning. *Methods in Ecology and Evolution, 6*(2), 198–208. https://doi.org/10.1111/2041-210X.12301

Davies, Z. G., Edmondson, J. L., Heinemeyer, A., Leake, J. R., & Gaston, K. J. (2011). Mapping an urban ecosystem service: Quantifying above-ground carbon storage at a city-wide scale. *Journal of Applied Ecology, 48*(5), 1125–1134. https://doi.org/10.1111/j.1365-2664.2011.02021.x

Duncanson, L., Rourke, O., & Dubayah, R. (2015). Small sample sizes yield biased allometric equations in temperate forests. *Scientific Reports, 5*(1), 17153. https://doi.org/10.1038/srep17153

Gholz, H. L., Grier, C. C., Campbell, A. G., & Brown, A. T. (1979, April). *Equations for estimating biomass and leaf area of plants in the Pacific Northwest*. Oregon State University. https://ir.library.oregonstate.edu/concern/technical_reports/bn999796n?locale=en

Greene, T. A., Reemts, C. M., & Appel, D. N. (2008). Efficacy of basal girdling to control oak wilt fungal mat production in Texas Red Oak (*Quercus buckleyi*) in Central Texas. *Southern Journal of Applied Forestry, 32*(4), 168–172. https://doi.org/10.1093/sjaf/32.4.168

Hutyra, L. R., Duren, R., Gurney, K. R., Grimm, N., Kort, E. A., Larson, E., & Shrestha, G. (2014). Urbanization and the carbon cycle: Current capabilities and research outlook from the natural sciences perspective. *Earth's Future, 2*(10), 473–495. https://doi.org/10.1002/2014EF000255

Jenkins, J. C., Chojnacky, D. C., Heath, L. S., & Birdsey, R. A. (2004). *Comprehensive database of diameter-based biomass regressions for North American tree species* (General Technical Report NE-319). U.S. Department of Agriculture, Forest Service. https://doi.org/10.2737/NE-GTR-319

Jenkins, J., Chojnacky, D., Heath, L., & Birdsey, R. (2003). National scale biomass estimators for United States tree species. *Forest Science, 49*(1), 12–35. https://doi.org/10.1093/forestscience/49.1.12

Jiang, M., Medlyn, B. E., Drake, J. E., Duursma, R. A., Anderson, I. C., Barton, C. V. M., Boer, M. M., Carrillo, Y., Castañeda-Gómez, L., Collins, L., Crous, K. Y., De Kauwe, M. G., dos Santos, B. M., Emmerson, K. M., Facey, S. L., Gherlenda, A. N., Gimeno, T. E., Hasegawa, S., Johnson, S. N., & Känaste, A. (2020). The fate of carbon in a mature forest under carbon dioxide enrichment. *Nature, 580*(7802), 227–231. https://doi.org/10.1038/s41586-020-2128-9

Jo, H.-K., & McPherson, E. G. (2001). Indirect carbon reduction by residential vegetation and planting strategies in Chicago, USA. *Journal of Environmental Management, 61*(2), 165–177. https://doi.org/10.1006/jema.2000.0393

Krooks, A., Kaasalainen, S., Kankare, V., Joensuu, M., Raumonen, P., & Kaasalainen, M. (2014). Predicting tree structure from tree height using terrestrial laser scanning and quantitative structure models. *Silva Fennica, 48*(2), 1125. https://www.silvafennica.fi/article/1125

Kükenbrink, D., Gardi, O., Morsdorf, F., Thürig, E., Schellenberger, A., & Mathys, L. (2021). Above-ground biomass references for urban trees from terrestrial laser scanning data. *Annals of Botany, 128*(6), 709–724. https://doi.org/10.1093/aob/mcab002

Lee, A., Jordan, H., & Horsley, J. (2015). Value of urban green spaces in promoting healthy living and wellbeing: Prospects for planning. *Risk Management and Healthcare Policy, 8*, 131–137. https://doi.org/10.2147/RMHP.S61654

Mascaro, J., Litton, C. M., Hughes, R. F., Uowolo, A., & Schnitzer, S. A. (2011). Minimizing bias in biomass allometry: Model selection and log-transformation of data. *Biotropica, 43*(6), 649–653. https://doi.org/10.1111/j.1744-7429.2011.00798.x

McDonald, R. I., Kroeger, T., Zhang, P., & Hamel, P. (2019). The value of US urban tree cover for reducing heat-related health impacts and electricity consumption. *Ecosystems, 23*(1), 137–150. https://doi.org/10.1007/s10021-019-00395-5

McHale, M. R., Burke, I. C., Lefsky, M. A., Peper, P. J., & McPherson, E. G. (2009). Urban forest biomass estimates: Is it important to use allometric relationships developed specifically for urban trees? *Urban Ecosystems, 12*(1), 95–113. https://doi.org/10.1007/s11252-009-0081-3

Morales, A., & MacFarlane, D. W. (2024). Reducing tree volume overestimation in quantitative structure models using modeled branch topology and direct twig measurements. *Forestry: An International Journal of Forest Research.* Advance online publication. https://doi.org/10.1093/forestry/cpae046

Nowak, D. J. (2024). *Understanding i-Tree: 2023 summary of programs and methods* (General Technical Report NRS-200-2023). U.S. Department of Agriculture, Forest Service. https://doi.org/10.2737/NRS-GTR-200-2023

Nowak, D. J., & Crane, D. E. (2002). Carbon storage and sequestration by urban trees in the USA. *Environmental Pollution, 116*(3), 381–389. https://doi.org/10.1016/S0269-7491(01)00214-7

Rahman, M. A., Stratopoulos, L. M. F., Moser-Reischl, A., Zölch, T., Häberle, K.-H., Rötzer, T., Pretzsch, H., & Pauleit, S. (2020). Traits of trees for cooling urban heat islands: A meta-analysis. *Building and Environment, 170*, 106606. https://doi.org/10.1016/j.buildenv.2019.106606

Raumonen, P., Kaasalainen, M., Åkerblom, M., Kaasalainen, S., Kaartinen, H., Vastaranta, M., Holopainen, M., Disney, M., & Lewis, P. (2013). Fast automatic precision tree models from terrestrial laser scanner data. *Remote Sensing, 5*(2), 491–520. https://doi.org/10.3390/rs5020491

Roxburgh, S. H., Paul, K. I., Clifford, D., England, J. R., & Raison, R. J. (2015). Guidelines for constructing allometric models for the prediction of woody biomass: How many individuals to harvest? *Ecosphere, 6*(3), Article 38. https://doi.org/10.1890/ES14-00251.1

Schick, M., Griffin, R., Cherrington, E., & Sever, T. (2023). Utilizing LiDAR to quantify aboveground tree biomass within an urban university. *Urban Forestry & Urban Greening, 89*, 128098. https://doi.org/10.1016/j.ufug.2023.128098

Shadman, S., Ahanaf Khalid, P., Hanafiah, M. M., Koyande, A. K., Islam, M. A., Bhuiyan, S. A., Kok, S. W., & Show, P.-L. (2022). The carbon sequestration potential of urban public parks of densely populated cities to improve environmental sustainability. *Sustainable Energy Technologies and Assessments, 52*, 102064. https://doi.org/10.1016/j.seta.2022.102064

Tanago, J. G. de, Lau, A., Bartholomeus, H., Herold, M., Avitabile, V., Raumonen, P., Martius, C., Goodman, R. C., Disney, M., Manuri, S., Burt, A., & Calders, K. (2017). Estimation of above-ground biomass of large tropical trees with terrestrial LiDAR. *Methods in Ecology and Evolution, 9*(2), 223–234. https://doi.org/10.1111/2041-210X.12904

Tavasoli, N., Arefi, H., Samiei-Esfahany, S., & Ronoud, Q. (2019). Modelling the amount of carbon stock using remote sensing in urban forest and its relationship with land use change. *The International Archives of the Photogrammetry, Remote Sensing and Spatial Information Sciences, XLII-4/W18*, 1051–1058. https://doi.org/10.5194/isprs-archives-XLII-4-W18-1051-2019

Tigges, J., Churkina, G., & Lakes, T. (2016). Modeling above-ground carbon storage: A remote sensing approach to derive individual tree species information in urban settings. *Urban Ecosystems, 20*(1), 97–111. https://doi.org/10.1007/s11252-016-0585-6

Torresan, C., Chiavetta, U., & Hackenberg, J. (2018). Applying quantitative structure models to plot-based terrestrial laser data to assess dendrometric parameters in dense mixed forests. *Forest Systems, 27*(1), e004. https://doi.org/10.5424/fs/2018271-12658

Wilkes, P., Disney, M., Armston, J., Bartholomeus, H., Bentley, L., Brede, B., Burt, A., Calders, K., Chavana-Bryant, C., Clewley, D., Duncanson, L., Forbes, B., Krisanski, S., Malhi, Y., Moffat, D., Origo, N., Shenkin, A., & Yang, W. (2023). TLS2trees: A scalable tree segmentation pipeline for TLS data. *Methods in Ecology and Evolution, 14*(12), 3083–3099. https://doi.org/10.1111/2041-210X.14233

Wolf, K. L., Lam, S. T., McKeen, J. K., Richardson, G. R. A., van den Bosch, M., & Bardekjian, A. C. (2020). Urban trees and human health: A scoping review. *International Journal of Environmental Research and Public Health, 17*(12), 4371. https://doi.org/10.3390/ijerph17124371